

Analysis of short-circuit transients in the LHC main dipole circuit

A Liakopoulou^{1,2}, A J Annema², L Bortot^{1,3}, Z Charifouline¹, M Maciejewski¹, M Prioli⁴, E Ravaoli¹, C Salm², J Schmitz² and A P Verweij¹

¹ CERN, Geneva, Switzerland

² University of Twente, Enschede, The Netherlands

³ Technische Universität Darmstadt, Darmstadt, Germany

⁴ INFN, Milan, Italy

E-mail: ak.liakopoulou@gmail.com

Abstract. After the occurrence and detection of a short circuit to ground in the LHC main dipole circuit, a fast power abort is triggered and the current in the circuit starts decaying semi-exponentially from a maximum value of 11.85 kA to zero, with a time constant of 103 s. If a short to ground occurs, the current flows through the fuse that is present in the grounding subcircuit. Depending on the value of the thermal load, the fuse first enters a pre-arcing region where it starts intermittently blowing up, until the blow-up threshold is reached, after which it definitively blows up. A simulation scheme utilising a common interface between PSpice and Matlab is proposed in order to simulate the blow-up behaviour of the fuse and hence increase the accuracy of the circuit model for short circuits to ground. A parametric analysis of the short circuit to ground parameters is performed and a better understanding of the behaviour of the circuit under different conditions is obtained. The worst-case values of the voltage to ground in the LHC main dipole circuit are identified for both the case where the intermittent behaviour of the fuse is included in the model as well as for the case where the fuse is not modelled and a comparison between the two is given.

1. Introduction

The Large Hadron Collider (LHC) spreads over a total distance of 26.7 km and comprises 8 sectors. In each sector there is one main dipole circuit, where 154 superconducting dipole magnets are connected in series [1]. Since 2007, there have been 19 occurrences of short circuit to ground faults in the superconducting LHC main dipole circuits, making their analysis and understanding necessary for the efficient operation of the accelerator. Each of the eight LHC main dipole circuits contain 154 superconducting magnets connected in series to a power converter. An equivalent model of the main dipole circuit developed in PSpice has been thoroughly analysed in [2] and the circuit schematic is presented in Figure 1.

In the figure, the superconducting dipole magnets are represented by inductors connected in parallel to a by-pass diode. However, in order to accurately model their nonlinear behaviour during transients, the more detailed model of Figure 2 is introduced [2]. In the model, the subcircuits of the two apertures Ap_1 and Ap_2 are connected in series, with a resistor R_p and the magnet's cold by-pass diode connected in parallel to both. The inductance of the apertures



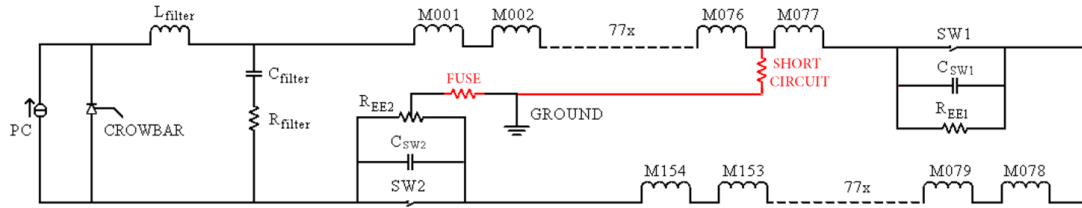


Figure 1. LHC main dipole equivalent circuit [2]. Added in red: 1) a resistor representing a single short circuit to ground between magnet M077 and ground, 2) a resistor representing the fuse in the grounding lines.

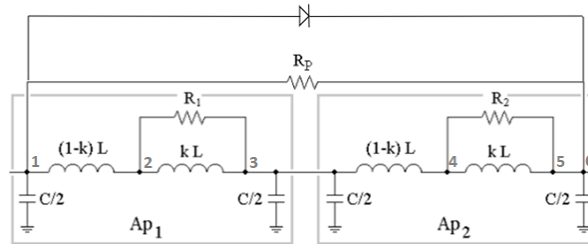


Figure 2. Circuit equivalent model of a LHC main dipole magnet [2].

is represented by L , while the capacitors C model the coil to ground parasitic capacitance. The inclusion of the factor k in the inductance values together with resistances R_1, R_2 achieve modeling of the induced eddy current effects. The values of these components have been calibrated in order to achieve the best match with the measured behaviour of the magnets and their values are equal to $L = 49$ mH, $R_p = 100$ Ω , $C = 150$ nF and $k = 0.75$ [2].

The main function of the power converter is to ramp the current in the circuit up to the nominal value of 11.85 kA at a linear ramp rate $\frac{dI}{dt}$ equal to $10 \frac{A}{s}$ [1]. The first crowbar, connected in parallel to the power converter, makes the circulation of the circuit current possible even after the latter switches off. The low-pass filter, that is also connected in parallel, has a cutoff frequency of 31.8 Hz and achieves the reduction of the high frequency noise introduced by the power converter [2]. The voltage waves propagating through the circuit following the switch-off of the power converter, are reduced by the second crowbar that follows the filter.

During normal operation, the current is ramped up to its nominal value by the power converter. After the switch-off of the latter, the current circulates without any resistance, since the circuit consists of superconducting magnets. However, in the case of fast transients occurring in the circuit, the non-linear behaviour of the various circuit elements lead to the appearance of transient effects that require thorough analysis and understanding. Common examples where these effects have been observed include fast power aborts (FPA) as well as faults appearing in the circuit [3]. A fast power abort consists of three distinct abrupt events, with the first one being the switch-off of the power converter. This is followed by the opening of two circuit switches, represented as $SW1$ and $SW2$ in Figure 1, which causes the energy extraction resistors R_{EE1} and R_{EE2} to become part of the main circuit loop [4]. The current starts decaying semi-exponentially with a time constant equal to 103 s, which is a function of the total inductance of the 154 magnets and the total resistance of the 2 energy extraction resistors.

The main dipole circuit is connected to ground through the grounding subsystem, presented in Figure 3. The exact connection is achieved at the intermediate point of resistors R_{EE2_3} and R_{EE2_4} , which together with R_{EE2_1} and R_{EE2_2} make up the equivalent resistance value R_{EE2} , shown in Figure 1. The circuit fuse can also be found in the grounding subcircuit and it has a

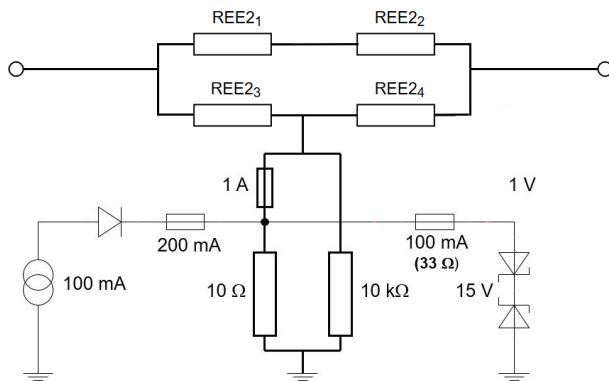


Figure 3. Grounding subcircuit including fuse, which achieves connection of the LHC main dipole circuit to earth.

resistance value equal to $1\ \Omega$.

The behaviour of the fuse is determined by the value of its thermal load. The thermal load is calculated as the time integral of the square of the fuse current over time, with the formula presented in equation 1.

$$ThermalLoad = \int I_{FUSE}^2 dt \quad (1)$$

The fuse reaches the pre-arcing threshold when its thermal load exceeds a value of $0.23\ A^2s$, while the blow-up threshold is reached when the value is higher than $1.2\ A^2s$. Current starts flowing through the fuse only after a short connection to ground has appeared, meaning that the integral has an initial value of zero at the time when the short occurs. Measured data revealed that in the pre-arcing region the fuse enters a state of uncertainty, characterized by intermittently blowing-up and recovering. After the blow-up thermal threshold is reached, it is considered that the fuse has definitively blown-up and can be modeled as an open circuit.

In this paper, the analysis is concentrated on the transients that occur during a single short circuit to ground. During such an event, a short connection appears between a magnet at a certain electrical position and ground. In the next section, the additions made to the PSpice equivalent electrical model of the LHC main dipole circuit, in order to simulate such an event are described. With an accurate model of the circuit behaviour during a short to ground event, the main goal of the study can be achieved, which is to identify the peak voltages to ground that can occur in the circuit.

2. Modeling Single Short Circuit To Ground

The simulation setup for a short to ground appearing in the circuit is analytically described in this section. A value of $11.5\ kA$ is considered as the maximum value of the current in the simulation, since it is the last point for which the ramp rate has the nominal linear value of $\frac{dI}{dt} = 10\ \frac{A}{s}$. The time when a fast power abort is triggered and the current of the power converter switches to zero, is set as the initial time point $t_0 = 0\ s$ of the simulation. The first and second energy extraction switches open approximately $350\ ms$ and $600\ ms$ respectively after the occurrence of the fast power abort [5].

A numerical simulation is performed and the short circuit position is chosen as magnet 70, meaning that resistance appears between the magnet at the specific electrical position and ground. To model the short circuit, a voltage controlled switch is added to the existing PSpice netlist model. By switching the voltage value from 0 to 1, a finite resistor is inserted in the circuit. A stimulus file is provided as input to the voltage controlled switch component, which contains a lookup table of the voltage values at discrete time points. A value of $1\ \Omega$ is chosen for the short resistance, which is set to a finite value at a time of $2\ s$ after the fast power abort,

when the transients caused by the latter have dissipated. This value is chosen as it represents a realistic possible value for a short circuit that appears in the circuit and the effect of different values will be discussed analytically later in the paper.

The plot of Figure 4 is presented first, where the voltages to ground of all 154 magnets are plotted over time. The signals are colorcoded, starting with blue for the voltage of magnet 1 and ending with red for the voltage of magnet 154. The time at which the fast power abort occurs, as well as the times when the energy extraction switches open, become visible in the same figure, as they are immediately followed by transient oscillations and a change of the magnet voltage polarities. Each event is followed by transient oscillations and it can also be seen that the polarities of the voltages change. After the appearance of the short circuit to ground at the time of 2s, the voltages of all magnets can be seen reaching higher peak values, after which they start decaying semi-exponentially to zero following the behaviour of the circuit current.

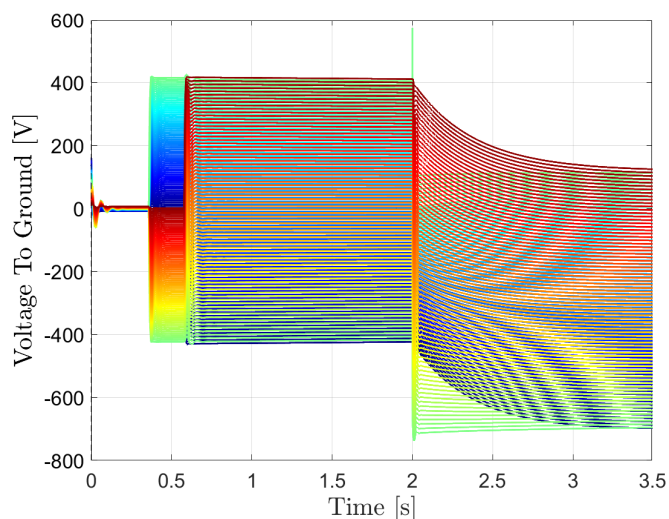


Figure 4. Simulated voltages to ground for all 154 magnets plotted as a function of time for the case when a single short circuit to ground appears in the circuit. The short circuit occurred between magnet 70 and ground at 2s with a short resistance of $1\ \Omega$.

Figure 5 is presented to observe the voltage to ground distribution at specific time points, following each event of the fast power abort. First, the time of 0.402 s is chosen, immediately after the transients caused by the first energy extraction have dissipated. With a resistance of approximately $73\ \text{m}\Omega$ and the circuit current value at the specific time almost equal to 11.5 kA, a voltage drop of about 800 V occurs over the resistor. This voltage drop becomes visible in the same figure as the difference in the voltage values obtained by the magnets in electrical positions 77 and 78, and is explained by the fact that the first energy extraction system is placed in the middle of the magnet chain. The polarity of the magnets with position numbers higher than 78 changes, due to the fact that the last magnet in the chain, which can be found at position 154, is connected to the second energy extraction resistor and hence obtains a value close to zero. For the time of 0.701 s, the second energy extraction resistor has also become part of the main circuit loop. This causes an additional voltage drop, observed in the figure between magnets 1 and 154, equal to approximately 800 V. Since the total voltage in the circuit is equally distributed over the 154 magnets of the chain, which have the same inductance value, in the case where both energy extraction resistors are active in the circuit, the voltage difference between two magnets is equal to about 11 V. For the time value of 4.027 s, a short with a resistance of $1\ \Omega$ has appeared at magnet 70, which causes the voltage of the magnet to decrease to a value almost equal to zero. This is observed in the figure by the voltage distribution curve shifting along the y-axis in order for this value to be obtained by the magnet between which and ground the short circuit appeared. Due to this shift, it follows that the highest voltages to ground are obtained when a

short to ground occurs at magnets 1, 77, 78 and 154, which are positioned on either side of the energy extraction systems.

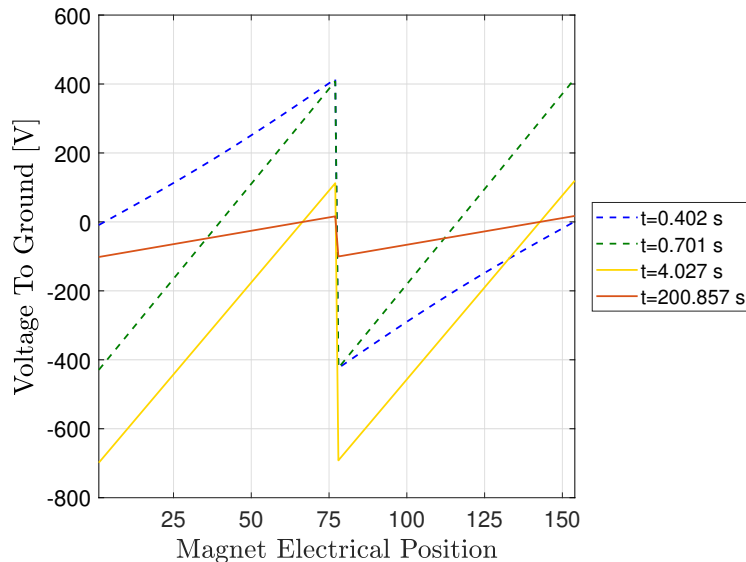


Figure 5. Simulated voltages to ground of Figure 4 plotted for specific time instances before (dashed line) and after (solid line) the short, as a function of the electrical magnet position. The voltage values are obtained from a simulation with a short to ground resistance of $1\ \Omega$ appearing between the magnet at position 70 and ground.

The voltage to ground distribution along the magnet chain is determined by several independent variables, namely the resistance of the short to ground and the magnet at which the short to ground appeared. Therefore, performing a parametric sweep for all 154 magnets where the short can occur and for 5 short resistance values with different orders of magnitude, namely 0.001, 1, 10, 100 and 1000 Ω , leads to the identification of the peak voltages to ground in the circuit.

The peak voltages to ground obtained for a short to ground with a resistance of $1\ \Omega$ occurring at different magnet positions, are presented in Figure 6. Peak voltage values of about 1.1 kV are observed for the magnets in electrical positions 1 and 30, when the short circuit appears between the magnets in positions 57 and 77. Voltage values of the same magnitude can also be seen for the magnets in positions 124 to 154 when the short occurs at magnets in all positions between 78 and 98. For all other cases, the voltages to ground do not exceed a value of approximately 0.9 kV.

When a short circuit to ground event occurs, current also flows through the fuse, that exists in the grounding subcircuit. The behaviour of the circuit during such an event can be modeled more accurately by including the blow-up behaviour of the fuse in the simulation. As was the case with the short to ground, a voltage controlled switch is chosen to model the switching behaviour of the fuse. Its intermittent blow-up behaviour can be included in the model, by providing the discrete time points at which the switch opens and closes in the form of a stimulus file as an input to the switch component.

A challenge remains however when trying to model the fuse blow-up behaviour accurately, since its state changes several times during a single simulation depending on the thermal load and consequently on the signal profile of the current flowing through it. A simulation scheme that utilises a common interface between Matlab and PSpice is proposed to achieve accurate modelling of the fuse behaviour and is explained next. First, the netlist of the circuit is solved by PSpice, from which the signal of the fuse current for the case when no blow-up occurs is obtained. The signal is numerically integrated in Matlab, in order to compute the thermal load as presented in equation 1. The time point at which the pre-arcing threshold is reached, is inserted next in the stimulus file, which is followed by the switching times of the voltage controlled switch, representing the pulses occurring during the fuse intermittent blow-up. A

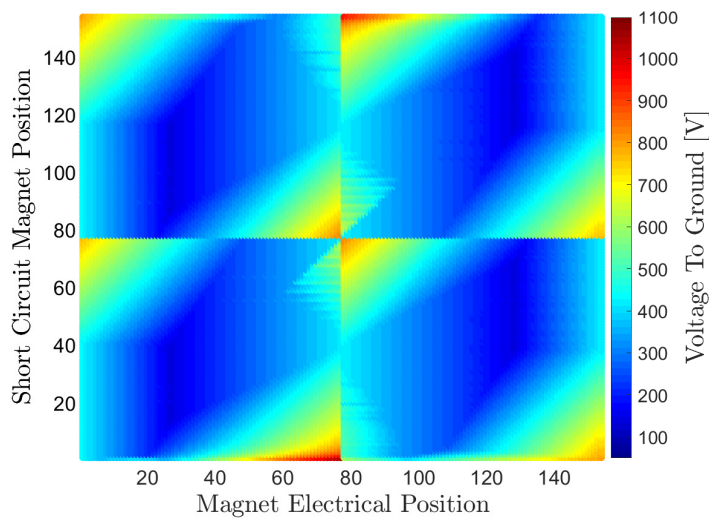


Figure 6. Peak voltage to ground values for a short resistance value of $1\ \Omega$ for the case when the fuse behaviour is not included in the model.

second simulation is performed and the signal of the fuse current is again obtained and integrated in Matlab. With the time point when the blow-up threshold of the fuse is reached found, its value is programmatically added to the stimulus file of the voltage controlled switch. A third and final simulation is then performed including the complete blow-up behaviour of the circuit fuse.

The current I_{FUSE} obtained from the simulation including the complete fuse blow-up behaviour is presented in Figure 7 together with the same signal obtained when the fuse behaviour is not modeled. For the latter case, the current through the fuse increases until a peak value of about 32 A, after which it decreases almost exponentially to zero. For the second signal of the figure, the intermittent blow-up behaviour of the fuse becomes easily distinguishable, with pulses starting at 2.042 s until the blow-up threshold is reached at 2.068 s.

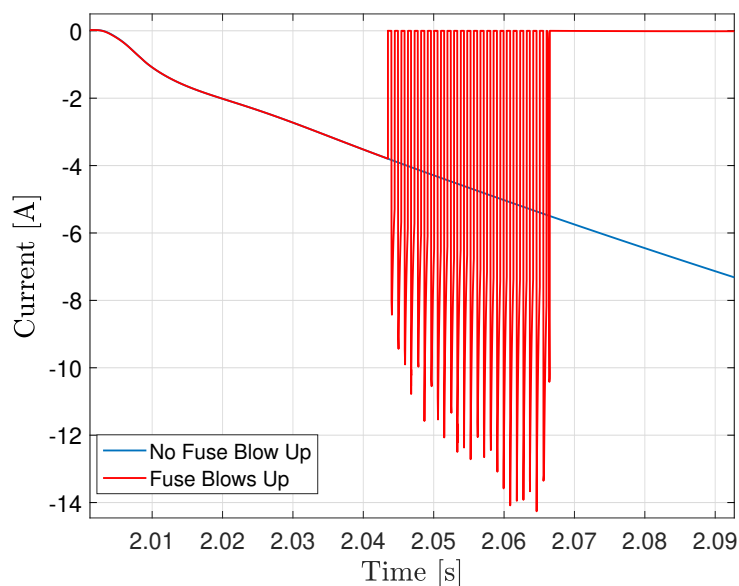


Figure 7. Comparison of simulated I_{FUSE} signal over time for a short circuit of $1\ \Omega$ occurring between magnet 77 and ground, for the simulation including the fuse blow-up behaviour and the case when the fuse does not blow up.

In Figure 8, the voltage behaviour for a window containing the times when the fast power abort and the opening of the energy extraction resistors occurred is presented. As was discussed for Figure 4, the times when these events occur become clearly visible as they are followed by

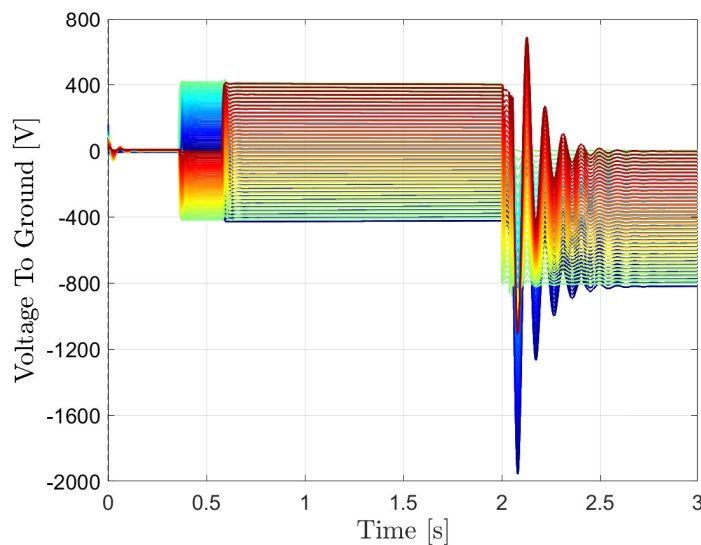


Figure 8. Simulated voltages to ground for all 154 magnets plotted as a function of time for the case when the intermittent behaviour of the fuse is included in the model. A short circuit occurs between magnet 77 and ground at 2s with a short resistance of $1\ \Omega$ and with the fuse blowing up.

transients. Following the time of 2s, when a short to ground appeared between the magnet in electrical position 77 and ground, large amplitude oscillations can be observed in the voltages to ground. The oscillations are damped, with the highest amplitude obtained right after the blow-up threshold is reached.

For the simulation with the short to ground resistance of $1\ \Omega$ appearing between magnet 77 and ground, the voltages to ground over the different magnet positions for specific times, are presented in Figure 9. A linear decrease is observed in the voltage values for the magnets in electrical positions following the position of the short circuit, in this case 77 to 154 for the times in between 2.04s and 2.102s. During the same times, the by-pass diodes in parallel to the magnets in the second half of the magnet chain, conduct. As a result, the voltage drop across each of these magnets becomes equal to the by-pass diode opening voltage of about 6 V. It can also be seen that the number of magnets for which this happens, is highest during the times when the first oscillation occurs and the peak amplitude is reached.

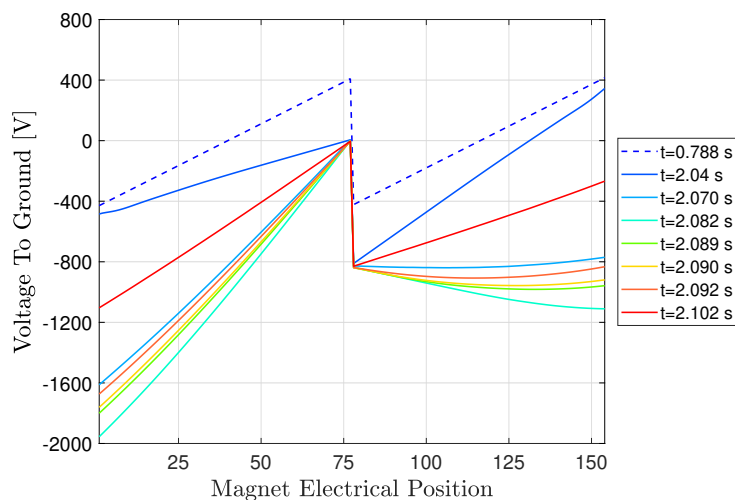


Figure 9. Simulated voltage to ground values plotted for specific times before (dashed line) and after (solid line) the short, as a function of the magnet's electrical position. The voltage values are obtained from a simulation with a short connection with a resistance of $1\ \Omega$ appearing between magnet 77 and ground.

3. Identification Of Peak Voltages To Ground

The same parametric sweep that was previously described for the values of the short position and resistance is also performed for the case when the fuse behaviour is modeled. In Figure 10 the peak voltage to ground values that can be reached by magnets of the LHC main dipole circuit for a short circuit resistance of $1\ \Omega$ are presented.

For a short circuit resistance values of $0.001\ \Omega$, $1\ \Omega$ and $10\ \Omega$, the colourplots containing the peak voltages to ground show only small deviations. As became clear in Figure 9, the voltage to ground reaches its highest values after the fuse has blown up and the current flows to ground through a $10\ \text{k}\Omega$ resistor, that is connected in parallel to the fuse. Since the equivalent resistance can reach values up to 3 orders of magnitude larger than the one obtained by the short circuit to ground, for the cases where the short resistance has a value smaller than $10\ \Omega$, different resistance values belonging in the aforementioned range do not cause a significant change in the peak voltages, which means that the colourplot of Figure 10 remains the same.

More specifically, for a resistance value of $1\ \Omega$ as well as all resistance values less than $10\ \Omega$, high voltages to ground are reached for magnets in positions 1 to 30 when short circuits occur between magnets 57 to 77 and magnets 124 to 154 for a short circuit in positions 78 to 98. For shorts circuits appearing at magnets between positions 30 to 40 and 110 to 120, it can be seen that irrespectively of the magnet electrical position, only small values can be obtained for the peak voltages. The middle range voltage values of about 0.8 to 1.3 kV are obtained by all magnets up to number 77 in the cases where a short appears at magnet positions 78 to 98 and magnets 78 to 154 when the short occurs between positions 57 to 77 and ground. The peak voltage to ground after the fuse blows up reaches an absolute magnitude of about 1.9 kV.

A comparison can be performed between the voltages to ground presented in Figure 10 with the voltages previously discussed in Figure 6. Although the same pattern for the peak values is observed in terms of the magnet positions, where the short appears, in the case where the fuse behaviour is not included, the peak values are almost a factor of two smaller than the peak values obtained for the simulations that included the blow-up behaviour of the fuse.

For the case when the short to ground resistance is equal to $100\ \Omega$, the voltages to ground in the circuit are significantly smaller when compared to the peak of 1.9 kV. The maximum value obtained in this plot is approximately equal to 1.2 kV for magnet 154 with a short occurring at position 78. The peak voltages are observed once again when the short appears at magnets 57 to 77 for magnets in positions ranging from 1 to 30, while for magnets at electrical positions 124

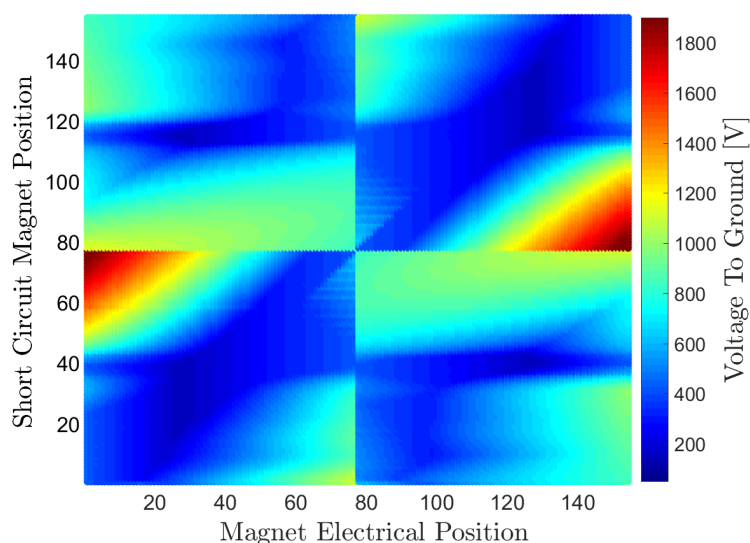


Figure 10. Peak voltages to ground for a short resistance value of $1\ \Omega$ for the case when the fuse blow-up behaviour is included in the simulation.

to 154, the largest voltage values appear when the short occurs at magnets 78 to 98. Mid-range voltage values are obtained for the magnets between positions 57 to 77 when a short appears at magnets 1 to 22 and 78 to 90. This is also the case when a short circuit appears at positions 57 to 77 and 140 to 154 for magnets at positions 78 to 98. Finally, voltages of the same range are observed for magnets in positions 1 to 22 for a short that occurs at magnets 140 to 154, as well as positions 140 to 154 for a short circuit at positions 1 to 20.

The same analysis follows for the case where the short circuit resistance is equal to 1 k Ω , with the difference that the voltages to ground obtain even smaller magnitudes and the peak voltages reach values of about 0.8 kV. For high resistance values, the current flowing through the short resistor is limited, which means that lower voltages to ground, are expected.

The analysis can be summarised in eight notable cases presented in Table 1. The table includes the peak values obtained for short circuit resistances smaller or equal to 10 Ω , where the worst cases are achieved. The table also acts as a quick reference for the voltage to ground obtained for specific magnets, by providing an analytical formula to calculate the peak voltages to ground value for different circuit parameters. For the equations presented in the last column of the table, R_{EE} represents the resistance of the energy extraction resistor, N_{MAG} the total number of magnets and V_D the forward voltage of the by-pass diodes.

Table 1. Cases of peak voltages to ground for $R_{SHORT} \leq 10 \Omega$

Notable Case #	Short Position	Magnet Position	Voltage Range	Peak Voltage
1	57-77	1-30	1.5 - 1.9 kV	$2R_{EE}I + \frac{N_{MAG}}{2}V_D$
2	78-98	124-154	1.5 - 1.9 kV	$2R_{EE}I + \frac{N_{MAG}}{2}V_D$
3	78-98	1-77	0.8 - 1.3 kV	$R_{EE}I + \frac{N_{MAG}}{2}V_D$
4	57-77	78-154	0.8 - 1.3 kV	$R_{EE}I + \frac{N_{MAG}}{2}V_D$
5	120-154	30-67	0.5 - 0.9 kV	$R_{EE}I$
6	1-35	45-77	0.5 - 0.9 kV	$R_{EE}I$
7	120-154	115-125	0.5 - 0.9 kV	$R_{EE}I$
8	1-35	100-140	0.5 - 0.9 kV	$R_{EE}I$

4. Discussion

Simulations show the worst-case voltage to ground in the LHC main dipole circuit could reach a value as high as 1.9 kV. Knowledge that such a high voltage to ground could be reached is important for the efficient protection of the circuit. It should be noted that the protection system currently installed in the circuit is capable of handling the voltage values in all observed scenarios. In fact, the circuits are routinely tested at voltage levels equal or higher than the simulated worst-case values, even in the case of an intermittent short circuit to ground. Furthermore, the probability of short-circuit occurrence will be reduced following the second LHC Long Shutdown, when the electrical robustness of components where short circuits to ground have been observed in the past, such as by-pass diodes and their connections, will be improved.

5. Conclusion

In this paper, the peak voltages to ground of the LHC main dipole circuit have been identified. The inclusion of the blow-up behaviour of the circuit fuse in the model has been achieved by creating a common interface that combines PSpice simulations and numerical calculations in

Matlab. The results of the simulations after performing a parametric sweep of the short circuit position and resistance value have been presented and a comparison has been provided with the case when the fuse behaviour is not included in the circuit. A value of about 1.9 kV has been determined as peak value for the circuit and is obtained for cases where the resistance of the short has a value less than or equal to $10\ \Omega$. When the short to ground resistance has a value larger than $10\ \Omega$, the peak voltages reach lower values. Additionally, it has been observed that regardless of the short resistance value, the highest voltage to ground values are obtained by the magnets in between electrical positions 57 to 77 as well as 78 to 98 for the cases where the short to ground appears between the magnets in positions 1 to 30 and 124 to 154 respectively. The paper concludes with the identification of three formulas from which the extreme voltages to ground can be computed for different combinations of short circuit resistance and magnet position.

References

- [1] Brüning O S, Collier P, Lebrun P, Myers S, Ostojic R, Poole J and Proudlock P 2004 *LHC Design Report* CERN DOI:10.5170/CERN-2004-003-V-1
- [2] Ravaioli E, Dahlerup-Petersen K, Formenti F, Steckert J, Thiesen H and Verweij A 2012 Modeling of the Voltage Waves in the LHC Main Dipole Circuits *IEEE Transactions on Applied Superconductivity* **22(3)** 9002704-9002704
- [3] Dahlerup-Petersen K and Bourgeois F 2001 Modelling and transmission-line calculations of the final superconducting dipole and quadrupole chains of Cern's LHC collider: methods and results *IEEE Conference Record - Abstracts. PPS-2001 Pulsed Power Plasma Science 2001. 28th IEEE International Conference on Plasma Science and 13th IEEE International Pulsed Power Conference (Cat. No.01CH37)* 213-
- [4] Dahlerup-Petersen K, Rodriguez-Mateos F, Schmidt R and Sonnemann F 2001 Energy extraction for the LHC superconducting circuits *Proceedings of the IEEE Particle Accelerator Conference* **5** 3448 - 3450
- [5] Ravaioli E *et al* 2012 Impact of the Voltage Transients After a Fast Power Abort on the Quench Detection System in the LHC Main Dipole Chain *IEEE Transactions on Applied Superconductivity* **22(3)** 9002504-9002504